Lawrence Berkeley National Laboratory

Bottom-up energy supply optimization of a national building stock

L. Kotzur[a,b] , P. Markewitz[a], M. Robinius[a], G. Cardoso[b], P. Stenzel[a], M. Heleno[b], D. Stolten[a].

[a] Institute of Electrochemical Process Engineering (IEK-3), Forschungszentrum Julich GmbH, Wilhelm-Johnen-Str., 52428 Julich, Germany
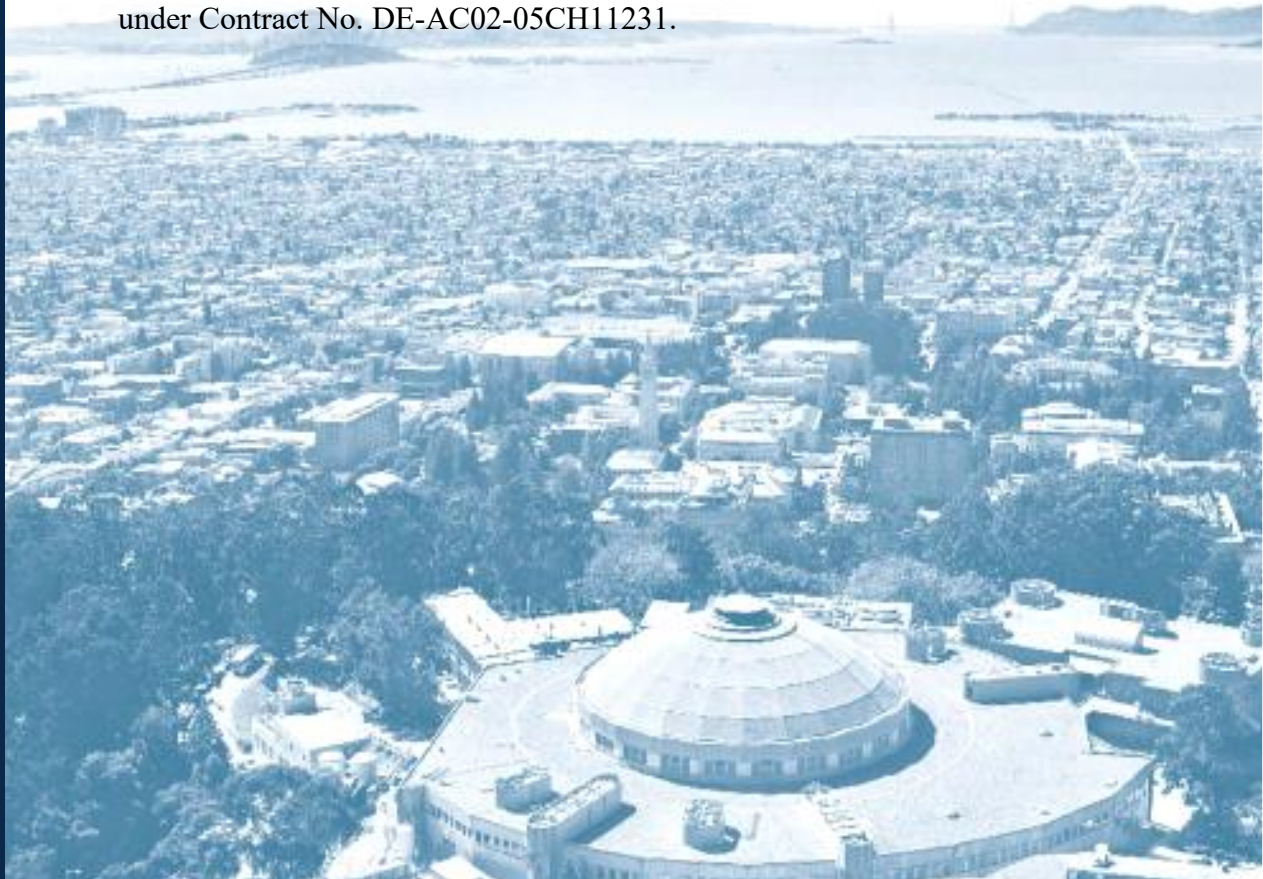[b] Lawrence Berkeley National Laboratory, University of California, 1 Cyclotron Rd, Berkeley, CA, USA
[c] Chair for Fuel Cells, RWTH Aachen University, c/o Institute of Electrochemical Process Engineering (IEK-3), Forschungszentrum Julich GmbH, Wilhelm-Johnen-Str., 52428 Julich, Germany

Disclaimer

Bottom-up energy supply optimization of a national building stock

Leander Kotzur[a,b,*], Peter Markewitz[a], Martin Robinius[a], Gonçalo Cardoso[b], Peter Stenzel[a], Miguel Heleno[b],
Detlef Stolten[a,c]

[a] *Institute of Electrochemical Process Engineering (IEK-3), Forschungszentrum Jülich GmbH, Wilhelm-Johnen-Str., 52428 Jülich,
Germany*
[b] *Lawrence Berkeley National Laboratory, University of California, 1 Cyclotron Rd, Berkeley, CA, USA*
[c] *Chair for Fuel Cells, RWTH Aachen University, c/o Institute of Electrochemical Process Engineering (IEK-3), Forschungszentrum Jülich
GmbH, Wilhelm-Johnen-Str., 52428 Jülich, Germany*

Abstract

The installation and operation distributed energy resources (DER), and the electrification of the heat supply, significantly changes the interaction of the residential building stock with the grid infrastructure, raising questions about its current design. Evaluating the mass deployment of DER at the national level would require analyzing millions of individual buildings, entailing significant computational burden.

To overcome this, this work proposes a novel spatially- and temporally-resolved bottom-up model. It consists of a single building optimization model to derive the future energy supply structure, and a novel aggregation algorithm to scale the technology adoption and operation to a nationwide scope by creating an archetype building stock from census data.

The model is validated for Germany, with 200 archetype buildings considered to sufficiently represent the diversity of the building stock. In a future scenario for 2050, photovoltaic and heat pumps are predicted to be the most economically and ecologically robust supply solutions for the different building types. Nevertheless, their electricity generation and demand temporally disjoin, resulting in a doubling of the peak electricity grid load in the rural areas during the winter. The urban areas can compensate this with efficient co-generation units, which are not cost-efficient in the rural areas.

Keywords: energy systems, archetype buildings, Mixed Integer Linear Programming (MILP), Zero Energy Buildings (ZEB), residential electricity demand

1. Introduction

1.1. Background

The residential building sector is responsible for 17% of worldwide CO_2 emissions [1]. In Germany, it was the source of 10% of the total Greenhouse Gases (GHG) through fossil fuel combustion in the year 2015. Moreover, it was responsible for 12% of total emissions due to the GHG footprint of its energy imports [2–4]. These emissions must be cut in order to reach the overall goal of net zero GHG emissions in the second half of this century [5] with the goal of minimizing the impact of anthropogenic climate change [6]. Therefore, the European Union introduced the concept of "Zero Energy Buildings" (ZEB) in the context of its energy performance of buildings directive [7, 8] with the goal of deploying GHG-neutral buildings that compensate for their emissions by exporting on-site generated renewable energy [9, 10].

While the objectives are clear, the pathway to GHG-neutral building stock is uncertain and the integration of new technological solutions unsettles utilities [11, 12] as well as governments [13]. Therefore, analyses are needed that predict technological development and their system integration: Many works for the building sector [14–18] solely focus on GHG reduction strategies for heat demand. They conclude that significant energy saving potentials can be accessed by increased refurbishment rates and that residual heat can be supplied with renewable energy.

Nevertheless, in relation to 'sector coupling' [19], the heat demand of the building sector can no longer be regarded as being more isolated from the other energy system: Heat pumps are seen as a key option to efficiently provide space heat [20, 21], while Combined Heat and Power (CHP) generation allows an efficient usage of chemical energy carriers while providing flexibility to the grid [22]. Furthermore, a trend towards an increased self-supply of residential buildings is apparent with the rapidly falling prices of photovoltaics [23] and batteries [24] constituting *grid parity* [25], meaning that the levelized cost of self-generated electricity is below the retail electricity grid price.

Both trends, i.e., the changing heat supply and the increasing self-sufficiency of the buildings, will significantly change the future grid load and challenge the feasibility of current electric grid design. Therefore, new analyses

---

*Corresponding author. Email: l.kotzur@fz-juelich.de

are required that consider the adoption and operation of new supply technologies and efficiency measures, predicting the spatially- and temporally-varying impacts on the grid infrastructure.

1.2. Related works

Various works have already performed top-down analyses of the load change due to single Distributed Energy Resources (DER), like photovoltaic [26], heat pumps and battery electric vehicles [27], or Combined Heat and Power (CHP) [28]. Seljom et al. [29] analyze the impact of photovoltaics deployed in ZEB in for the future Scandinavien energy system. Nevertheless, as demand, flexibility options and generation are closely connected to the building supply systems, these technologies can not be evaluated independently and must be get holistically regarded and modeled as system entities. This can primarily be done by means of detailed bottom-up models that simultaneously consider investment decisions and the operation of DER as well as efficiency measures and demand side management.

1.2.1. Single building optimization

Thereby, the models must account for cost optimality, as the main motivations of building owners to adopt different supply technologies are savings or earnings emanating from their installation [30]. This also applies for the efficiency measures or energy retrofits, where the need of replacement or financial profitability are the main activators for the adoption [31].

Therefore, many different optimization models have been proposed for determining the cost optimal investment decisions and operation of single building supply systems: either as Linear Programs (LP) [32, 33] with the advantage of good computational tractability but the disadvantage of not being able to account for economies of scale; or as a Mixed Integer Linear Program (MILP) model [34–40]. Furthermore, two-level approaches that determine at least a part of investment decisions with a meta-heuristic solver and operation with a simulation or optimization are popular [41–46]. The last approach can account for very detailed physical models. but no optimal solution is guaranteed. Some of the models even include the investment

decision into efficiency measures due to adapting the envelope in the investment decision [42, 46–48].

All models would enable the analysis of the impact of technology adoption and operation on the local infrastructures: for instance, Lindberg et al. [38] apply a MILP to design the supply system of a Multi-Family-House (MFH) and analyze the resulting electricity grid load for cost-optimal system operation under current German regulations. Schütz et al. [40] use a model to evaluate the optimal technology adoption with currently considered incentives and market conditions for the case of three reference buildings.

1.2.2. Archetype buildings

Although these analyses and models already provide many insights for the application cases, a further generalization would be required to upscale these results to an aggregated nationwide perspective. Furthermore, the spatial variation due to regionally differing building topologies would be required to integrate the results to grid models. Therefore, a set of representative buildings is required that characterizes the spatial diversity of building stock and that can be used for the previously described single building models.

In general, such typical buildings are often referred to as *archetype buildings* and are commonly used for modeling GHG reduction strategies in the building sector [49], as described in the Energy Performance of Buildings Directive [7, 8] of the *European Union*.

In this context, Corgnati et al. [50] introduced different pathways to determine representative reference buildings for the analysis of cost optimal refurbishment measures, but conclude that in reality most often a mixture is used due to the different available data for different buildings stocks.

Mata et al. [51] proposed an analytical methodology to aggregate archetype building stocks based on publicly available data. The steps include a *segmentation* based on categories such as construction year, a technical *characterization* such as the thermal transmittance as input values for energy performance models, as well as a *quantification* to scale the buildings up to a nationwide level.

The methodology is applied to France, Germany, Spain, and the UK, with the resulting final energy demand showing a deviation of less than -4% to + 2% to the aggregated statistical values.

Various nation-specific works exist to quantify the energy consumption of the building sector with the help of archetype buildings: the German residential building stock is described by a framework developed by the *Institute für Wohnen und Umwelt* (IWU) [52, 53]. This schema categorizes the stock into classes that differ by construction year and building size that are represented with detailed technical parameters. This stock description has been extended to other European countries in the framework of the *EPISCOPE* project [54]. The US *Department of Energy* (DOE) introduced archetype buildings for the residential sector [55] and the service sector [56] in the USA, referred to as benchmark or prototype buildings. An advantage over the European database [54] is the fact that additional time series data are provided for the different building demands, including electricity, hot water, cooling or heating demand for typical days in different climate zones.

The aggregation to archetype buildings is also widespread in the context of urban energy models: Dall'O' et al. [57] present a work flow to derive archetype buildings with a combination of statistical data and a survey applied to sample buildings. Meanwhile. Cerezo et al. [58] and Sokol et al. [59] introduce methods to estimate unknown attributes of the proposed archetype buildings, such as comfort temperature levels, based on a probability distribution. This approach can make use of measured energy data in different buildings, such as annual or monthly gas demand, and fits the uncertain attributes to it. Moreover, Fazlollahi et al. [60] and Fonseca and Schlueter [61] use k-means clustering methods to group similar buildings in urban areas by using the location of the buildings and spatially resolved statistics. The advantage of clustering is that the simulation models or optimization models can be applied to the zones instead of the single buildings, which reduces the number of variables and the computational load of the related models.

1.3. Own approach and structure

In summary, many works exist that consider detailed integrated single building optimization models to determine the cost optimal technology adoption and operation. There also exist many different approaches for the aggregation and segmentation of archetype buildings. Nevertheless, to the knowledge of the authors their integrated combination for the purpose of analyzing the spatially and temporally changing demand of the infrastructure, i.e. gas grid and electricity grid, does not exist.

Therefore, this work proposes a framework to describe a spatially resolved building stock with a limited number of archetype buildings. Those buildings can be optimized under different regulatory regimes in order to derive their future technology installation and operation. Their spatial assignment allows for the local evaluation of the changing energy demand. The general idea is visualized Figure 1. Thereby, a sufficient number of archetype buildings are required to describe the geographically resolved variation of the real building stock that affects the grid load at different nodes in the electricity grid. At the same time, the number of archetype buildings is limited due to the computational load of determining the optimal retrofit and DER adoption of each building archetype. A trade-off between model representativity and complexity must be made, wherefore the building aggregation must be flexible enough to be adapted to the available computational resources and the required degree of detail.
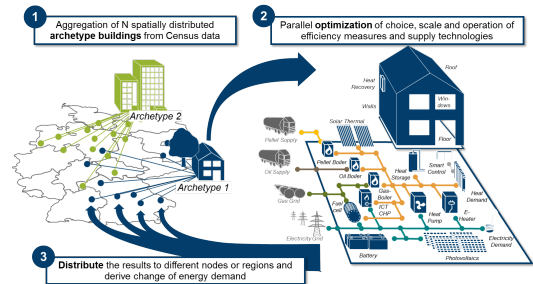
Figure 1: Structure of the bottom-up model to optimize the a spatially resolved building stock and determine the changing infrastructure usage.

In general, the two modules, consisting of the spatially-resolved building aggregation and the single building optimization, should be replaceable. As concluded by Corgnati et al. [50], the aggregation and descriptions of the archetype buildings is highly dependent on the available data. The algorithm in this work is tailored for the data structure of the German Census [62] that describes the statistical distributions of building parameters at the municipality level. The data is also available at a granular grid of 100m [62], making the aggregation algorithm and with it the whole model chain applicable to single urban areas.

With the help of this modeling approach the potential for self-sufficient energy supply systems in residential buildings can be efficiently evaluated and its large-scale techno-economic impact on the grid load derived. To do so, Section 2 introduces the used aggregation tool, the used data sets and the single building optmization for this model. The bottom-up model is applied for a reference scenario in Section 3 and validated to the available aggregated energy demand data. In order to derive the changing load, a future supply scenario is introduced in Section 4 for the year 2050. Section 5 critically recaps the work and draws the main conclusions.

2. Methods and data

The model consists of two main components:

3

1. The single building optimization, described in Section 2.1, represents the decision making of the building owner regarding the design and operation of the energy supply.

2. The aggregation and distribution of archetype buildings, introduced in Section 2.2, makes the single building optimization results generalizable to the perspective of regulators and grid operators on a nationwide scale.

2.1. Single building optimization

The single building optimization is based on a typical Mixed-Integer Linear Program (MILP) with the objective of minimizing the annual energy cost of a single building as proposed in the vast literature. The operation and design of the supply system is modeled with the object-oriented system modeling framework FINE [63–65]. The binary variables are considered to sufficiently incorporate the economy of scale of the technologies. The operation is modeled in a fully linear and continuous manner.

The heat load is considered with the 5R1C-model from EN ISO 13799 [66], which was implemented into a MILP by Schütz et al. [48]. The physical building properties, such as heat transfer coefficients for different construction years are taken from IWU [53]. This is able to account for the thermal building mass for a flexible supply system operation. Furthermore, potential refurbishment measures are part of the solution space, such as the addition of wall or roof insulation, the replacement of windows, or the integration of smart thermostats. The configuration of the buildings is introduced in detail in Kotzur [64].

The occupancy behavior and inherited electricity load of the appliances are created with the help of the CREST demand model [67–70]. The advantage of this model is that it sufficiently incorporates the high variance of single residential load profiles, as well as the stochastic smoothing for the case that an agglomeration of households is considered. A validation of the model in the context of German residential electricity demand is performed in Kotzur [64] and exhibits sufficient accuracy.

The time series for PV and solar thermal are created with the PV-Lib [71]. The weather data is derived from the DIN EN 12831 [72] by finding the closest location listed. Therefrom, the minimal design temperature is derived as well as the test reference region of the *Deutsche Wetter Dienst (DWD)* [73]. Alternatively, the weather from the COSMO rea-6 reanalysis data set [74] is used for real weather years for validation purposes.

All in all, the combinatorial consideration of demand-side and supply-side measures yields a complex mathematical program that is computationally demanding. In order to keep the program tractable for many different building types and scenarios, the annual time series of weather, occupancy behavior, and appliance load are aggregated to twelve typical days with a hierarchical aggregation [65, 75]. The days with the smallest temperature and highest electricity load are added as extreme days. Based on these, the optimal choice of the supply technologies and refurbishment measures is determined with the MILP. The binary decision variables are then fixed and a validation and scaling optimization is then performed for the full annual time series [76], similar to that in Bahl et al. [77].

The detailed model description and their independent validation can be found in Kotzur [64].

2.2. Aggregation of archetype buildings

In the following, the aggregation of a spatially-distributed archetype building stock is presented. These are used to scale the results of single building optimizations to a spatially-resolved nationwide perspective. Therefore, Section 2.2.1 discusses the relevant attributes to describe the energy performance of a building. The aggregation algorithm is sketched in Section 2.2.2 and its application is illustrated in Section 2.2.3.

2.2.1. Relevant building attributes

In general, four categories of building attributes are emphasized in the literature, while the concrete nomenclature varies [50, 51]: The *Form* describes the physical exterior shape of the building, including orientation, wall area, window area and roof areas. The *Envelope* characterizes the physical properties of the materials used in the building. The technologies installed in the buildings to satisfy thermal comfort and other demands are grouped into the category of *System*. *Operation*, in turn, summarizes all extrinsic conditions determining the system operation, such as the local weather or occupancy behavior.

Aside from the attributes describing the current energy performance, future energy supply is also of interest, where the category of *Adoption* summarizes all attributes referring to the investment capabilities and investment behavior of the building owner, such as a potential interest rate. For instance, the model described here considers the cost-optimal technology adoption of the different buildings.

The categories and their aggregation define a general framework to segment buildings, but the required attributes depend on the model and data availability, e.g., the envelope could be described by materials with exact heat conductivities and thicknesses, only heat transfer coefficients, or by the construction year of the building from which these values are derived.

The attributes considered for the aggregation procedure of this work are oriented towards the model introduced in Section 2.1 and the data provided by the census [62]. Figure 2 shows the aggregated Census data for Germany. The total number of buildings is predominated by over 12.3 million Single-Family Houses (SFH) and 6.3 multi-family houses, while buildings with more than 12 apartments have, at 0.21 million, a small share at the total number. The majority of the SFH are detached, constituting an overall small proportion of terraced and semi-detached buildings. 23.2 million of the 40.5 million apartments are rented, while one- and two-person households

4

dominate with together 27.1 million households. These also constitute the peak of apartment sizes, with compact living areas of 59 to 79 m² per household, while larger single-family houses are spread over a larger grouping.
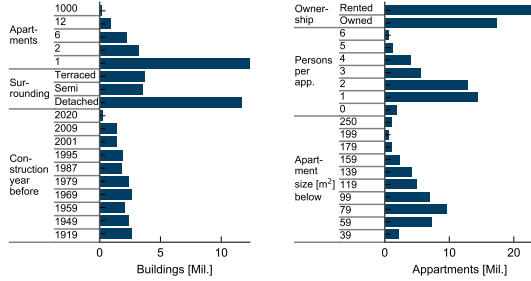

Figure 2: Attribute distribution of the German residential building stock based on the Census [62].

All of these distributions are also available on an absolute scale for the municipalities or a 100m grid in Germany and state the data basis for the considered archetype aggregation, as shown in Figure 3. The introduction of additional values is discussed in detail in Kotzur [64].
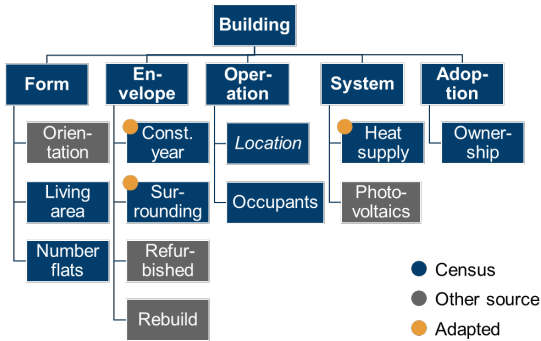

Figure 3: Structure of the considered attributes relevant for the building energy supply.

2.2.2. Building aggregation algorithm

These attribute distributions must be aggregated to a limited set of archetype buildings to evaluate them energetically.

In general, the attributes belonging to the different categories are primarily published as aggregated distributions for different administrative boundaries that define the spatial resolution. Nevertheless, the concrete building instances and their values are unknown wherefore cross-combinations of attributes are not reproducible, e.g., how many terraced buildings have a certain living area.

Thereby, two challenges arise: first, the buildings are described by a mixture of categorical and continuous attributes. Approaches exist dealing with this type of aggregation class, such as the mixture of *k-means* and *k-modes* clustering, referred to as *k-prototypes* [78]. Nevertheless,

these would rely on a data set consisting of real building instances that should be clustered and can then be represented, e.g., by its medoid. This does not apply to the attributes distributions, and so a new aggregation methodology is required that is introduced in Kotzur [64].

Thereby, a greedy algorithm is introduced with the goal of determining a locally optimal set of archetype buildings. It is inspired by the concept of an expectation-maximization algorithm, where Lloyd's k-means clustering algorithm [79, 80] and the k-prototypes algorithm [78] belong as well.
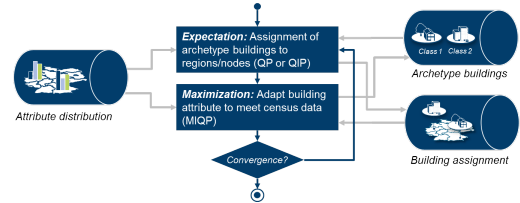
Figure 4: Structure of the developed algorithm to determine a spatially distributed archetype building stock.

The idea is to describe the assignment of the archetype buildings to the different nodes or municipalities as the *expectation* step, with the objective of getting a representation of the attribute distributions by the most likely archetype buildings into every municipality. Nevertheless, the attributes of the archetype buildings themselves are unknown, and so their estimation is defined as the *maximization* step, illustrated in Figure 4. This results in two optimization problems that are iteratively solved.

The result is a set of archetype buildings and a matrix that defines the representation of every municipality by the number of certain archetype buildings.

2.2.3. Application and illustration of the results

The initial guess of the archetype building attributes, the start solutions for the algorithm, are derived from the current state of the art archetype buildings for Germany [53], while missing parameters are randomly generated, e.g. the number of persons living in an apartment.

In the ollowing, the algorithm is applied once to different predefined numbers of archetype buildings in order to determine how many of these are required for a sufficient representation of the German building stock.

The quality of the resulting representation of the different attributes for different numbers of archetype buildings is illustrated in Figure 5. This is defined as the cumulative deviation of the representation of an attribute expression m for every region in proportion to the total attribute manifestations for the whole of Germany:

$$f(p,m) = \frac{\sum_{n \in N} d_{n,m,p} - \left| d_{n,m,p} - \sum_{b \in B} \beta_{b,n} \delta_{b,p,m} \right|}{\sum_{n \in N} d_{n,m,p}} \quad \forall \quad p,m \tag{1}$$

The figure shows that for some of the attribute expressions, a small number of archetype buildings are able

Figure 5: Relative fit of all categorical attribute expressions for different numbers of archetype buildings in Germany.

is spreading, as similar categorical building types can be instantiated multiple times. For the case of 800 archetype buildings, it is even observable that urban areas are represented by more archetype buildings than rural areas.

Figure 6: Geographical location of different numbers of archetype buildings in the final iteration step.

to represent them sufficiently, for instance single-family houses with a single apartment or the energy supplied by gas boilers. These are attribute expressions that often occur in the original data set. Therefore, they are first rep-
395 resented by the archetype buildings to reduce the overall error. Nevertheless, attributes such as a CHP, heat pump supply, or apartments with a living area smaller than 39 m^2 rarely occur in the Census data set. Therefore, the algorithm has a secondary priority to represent them and
400 focuses instead on building attributes that exist more often, e.g., no archetype building was created with a heat pump supply for 5, 25 and 50 archetype buildings because the overall share of heat pump supply in Germany is below 2 %. Thus, it would not be efficient to sacrifice an
405 additional archetype building to represent it.

In general, this is to clarify that a fit below 100 % does not imply that the expression is highly under-represented on the aggregated level: While an overestimation of an attribute in one region and an underestimation in the other
410 regions constitute a reduced fit, they could add up and compensate each other on an aggregated nationwide level, which is further elaborated in Kotzur [64].

The fitting of the continuous attributes, the latitude and longitude, is qualitatively illustrated in Figure 6 with
415 their exact geographical placement in Germany. For the case of 5 to 25 archetype buildings, all buildings are primarily located in the center of the country. The reason is that building archetypes are mainly used to represent the diversity of categorical attribute combinations that
420 are spatially distributed across Germany. E.g., a single-family house from 1960 with a four-person household and gas boiler supply manifests as an archetype building that represents this building type in the north as well as in the south. For higher numbers of archetype buildings from 100
425 to 800, the geo-spatial location of the archetype buildings

The representation of municipalities is further illustrated in Figure 7, which introduces the local assignment
430 to the different municipalities of certain example archetype buildings, selected from the set of 800. The locations of the archetype buildings are the centers of the buildings they represent in the different municipalities. As these representations are spatially spread over different munici-
435 palities, the archetypes are not placed at municipalities at the border.

Furthermore, it is recognizable that the areas and amounts that are represented differ between the archetypes: While an archetype building supplied with heat pumps must rep-
440 resent buildings over a large area, archetype single-family houses supplied by gas boilers have a definite local assignment area. The reason for this is that more archetype buildings with gas boilers are selected, as more buildings with gas boilers also exist in reality. Therefore, the algo-
445 rithm chooses a higher spatial separation for them to minimize the overall error, while accepting a higher geospatial estimation error for the few buildings with heat pumps.

3. Validation of the method

450 This section applies the single building optimization introduced in Section 2.1 to the archetype buildings aggregated in Section 2.2.3. The choice of the technologies
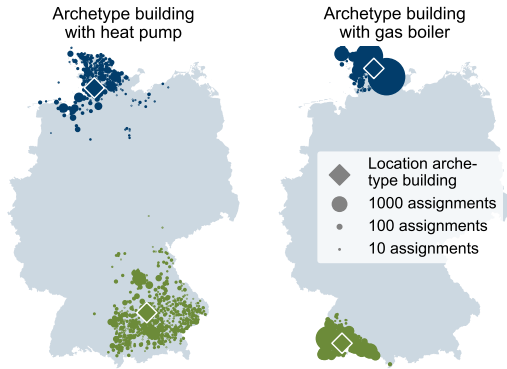
Figure 7: Location of the most northern (blue) and most southern (green) single-family house archetype with heat pump supply (left) and gas boiler supply (right) of the set of 800 archetype buildings, and their assignment to the different municipalities.

are predefined by the archetype definition [64], but the technology scale and operation are optimized such that the building-specific energy demands are met. It defines the *Reference* status quo of the residential energy supply and validates the model to national energy demand statistics. The techno-economic assumptions are introduced in Appendix A.

First, Section 3.1 shows the impact of choosing different numbers of archetype buildings on the resulting final energy demand and concludes a sufficient number of archetype buildings for further scenarios. The effect of different weather years on the energy performance is compared in Section 3.2.

3.1. Impact of the number of archetype buildings

The different numbers of aggregated archetype buildings introduced in Section 2.2.3 are independently optimized for the status quo and then multiplied with their appearance in Germany.

The resulting final energy demands are aggregated to different energy carriers and illustrated in Figure 8. They are validated against the final energy demand provided by AGEB [2].
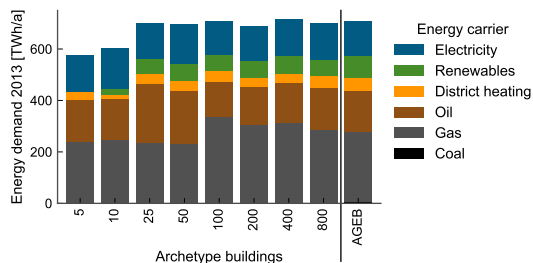

Figure 8: Final residential energy demand predicted for different numbers of archetype buildings.

The dominant energy carriers for the residential sector are gas, oil and electricity with 268, 162 and 136 TWh/a

per year [2]. The demand for renewable energy or district heating is secondary with 84 and 51 TWh/a per year. As can be seen in Figure 8, the model is able to roughly predict with five to ten archetype buildings the demand of the three dominant energy carriers, but the appearance of minor energy supply carriers is not sufficiently included. This improves with an increasing number of archetype buildings while the best fit can be achieved with 800 buildings. Nevertheless, the resulting demands of 64.8 TWh/a for renewables and 44 TWh/a for district heating are still underestimated. This deviation is constituted by the aggregation, which tries to capture the most frequently appearing archetype buildings and neglects rarely occurring building types. Nevertheless, these missing energy demands for renewables and district heating are compensated by gas and oil demands, which are slightly overestimated with 286 and 165 TWh/a. This compensation effect already appears for 25 archetype buildings, where all cases between 25 and 800 archetype buildings predict the total final energy demand in a similar magnitude as the AGEB [2]. Above 200 archetype buildings, the share of the different energy carriers also aligns well with the structure of the AGEB [2].

The prediction with 50 archetype buildings overestimates the demand for oil by 27.4% and underestimates the demand for gas by 17.1%, while 100 archetype buildings on the contrary overestimate the gas demand by 25.5% and underestimate the oil demand by 16.1%. This switch shows a drawback of the aggregation: Some archetype buildings appear often and therefore have a high impact on the overall energy load. If the majority of the buildings supplied, e.g., with gas boilers have a construction year before 1960 while the more modern buildings are supplied with oil, an overestimation of the gas demand and an underestimation of the oil demand results, although the absolute number of the different boiler types is well represented. Nevertheless, this effect is reduced with an increasing number of archetype buildings, as single archetypes represent attribute distributions on a more granular level. In consequence, the spatial differences, e.g., of construction years, are better fitted and intrinsic correlations of the input data are represented with higher accuracy.

This work assumes 200 archetype buildings as a sufficient trade-off between accuracy and computational load, since they already capture the main diversity of the energy carriers and the statistical balancing effects between the buildings.

3.2. Impact of different weather years

The following section evaluates the impact of different weather years on the energy demand of the buildings. The resulting final energy demands for the weather years 2010 to 2015 and the Test Reference Year (TRY) are illustrated in Figure 9 for 200 archetype buildings and validated again to the final energy demand values provided by AGEB [2]. According to AGEB [2], the total residential energy de-

mand varies from 743 TWh in 2010 at a maximum to 608 TWh for 2014 as a minimum.
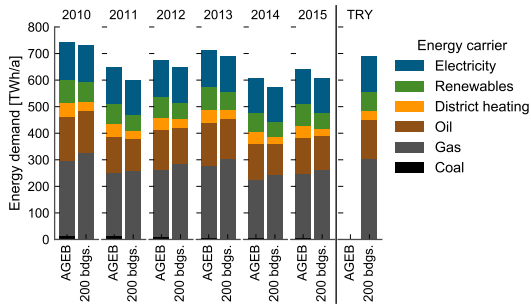

Figure 9: Final energy demand for different weather years predicted with 200 archetype buildings and compared to the values reported by the AGEB [2].
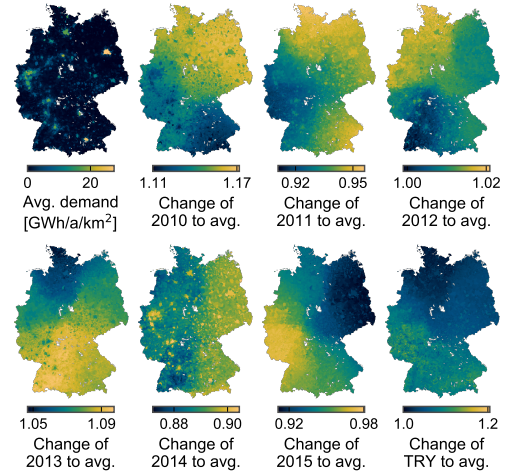

Figure 10: Spatial distribution of the final energy demand, averaged for the considered years 2010 until 2015, and the relative regional deviation from the average value.

For all different weather years, the systematic overestimation of gas demand and underestimation of district heating demand is observed, as already discussed in the previous section. Nevertheless, the relative deviation differs between the years. While the total final energy demand fits well for 2010 with an underestimation of below 2%, the deviation increases in the year 2011 up to 7.4%. It reduces again to 2.8% in the year 2013 while 2014 again has a value of 5.8%. The differences are mainly constituted by the different demands for the energy carriers that are used to supply the space heat, while the electricity demands remain almost constant for all periods. It seems that in relatively mild weather years, the deviation is higher than in colder weather years. A probable explanation of the varying deviations could be an adaptive occupancy behavior, e.g., the ventilation rates could be reduced in colder winters, which is not taken in to account in the model.

Figure 10 shows the spatial distribution of the final energy demand averaged for all of the weather years considered. It clusters in the cities as expected. Additionally, the relative changes of the final energy demand for the different weather years are illustrated for the different municipalities. The overall magnitudes of the differences align with the differences shown in Figure 9. Nevertheless, it is clearly recognizable that different weather years spatially impact the annual energy demand spatially differently: While the year 2010 was generally a cold year, in northern Germany the final energy demand was 17% above the average while in south-west Germany it was only 11% higher than the average. This is the opposite to 2013, when Southern Germany's energy demand was 9% above the regional average, while northern Germany lies just 5% above the average. This highlights the importance of having a spatially resolved building stock model, as a single location is not able to represent this variation sufficiently.

In 2014, no significant differences due to the geo-position are observed. Nevertheless, it becomes clear that the cities are less sensitive to the weather patterns (11.5% below the average in 2014) than the rural areas (13.5% below the

average in 2014). The reason is that the relative share of energy demand for space heating to the overall energy demand is smaller in the cities than in the rural areas, reducing the relative impact of weather years on the total energy demand.

The analysis illustrates that the novel spatially resolved approach is able to identify local extreme weather patterns. While it was only shown here for the aggregated annual demand, the model also predicts the temporal demand of the energy carriers in all municipalities and can be used for the identification of local peak demands that are relevant for the infrastructure's design.

4. Future energy supply scenario

This section presents the cost minimal residential energy supply structure for the year 2050 under the assumption of a *homo economicus* and analyzes the value of different technologies for the overall energy supply, the impact of an increased refurbishment rate and the sensitivity to the considered gas price.

In order to predict the change of the supply structure in the future, the overall model is applied to 200 archetype buildings for the techno-economic assumptions in 2050, which are defined in Appendix A.2. It is implied that the building owners have a technology adoption and operation approach that minimizes their energy cost. The choice, scale, and operation of the considered energy supply technologies are optimized together with the heating system and potential refurbishment measures. The cost for envelope refurbishment measures differs between buildings that are in the refurbishment cycle and buildings that are not, as discussed in detail in Kotzur [64]. Existing heating technologies are assumed to get replaced until 2050. The results define the overall state that the residential energy supply system is converging on if the assumed en-

ergy prices and the techno-economic assumptions for the technologies arise. Besides the incentives included in the scenario, no additional ones are given by regulators. The demand for the use of electrical devices, hot water demand and thermal comfort level are asumed to stay the same as in the *Reference* scenario, which refers to the status quo described in Section 3 with the assumptions described in Appendix A.2.

The resulting system design is shown and discussed in Section 4.1 for the aggregated nationwide perspective as well as for single archetype buildings. Section 4.2 points out the spatial and temporal changes of the grid load due to the changing energy supply. The value of different technologies for the energy supply or the impact of higher refurbishment rates are analyzed in Section 4.3.

4.1. Design and costs

The total expenditures related to investments in the supply structure or energetic refurbishment measures are visualized in Figure 11. The aggregated capacities and energy flows are shown in Appendix B. To realize the technology portfolio, an overall investment of 382.3 billion Euro is needed. The largest share is photovoltaics, with a total investment of 104.6 billion Euro and a total capacity of 133.4 GW. 89.7 TWh/a of the generated electricity is used for self-consumption, which is the main incentive to deploy photovoltaic.

The second highest investment is for heat pumps with 88 billion Euro indicating that these are the main supplier of space heating. Fuel cells are the chosen flexible co-generation option and amount to 5.4% of the annual costs. The heat storage systems make up 1.9% of the annual costs and have a total investment of 21.8 billion Euro. The investment in the batteries is significantly lower with 6.9 billion Euro, amounting to 1% of the annual costs. The log wood supply for the fireplaces amounts to 2.1%, while the electric heaters have a minor share. District heating, oil boilers and pellet boilers are not chosen in the solution, as they are not competitive in comparison to the heat pumps or gas boilers.
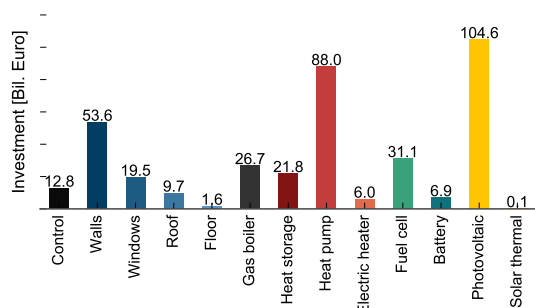
Figure 11: Total investments into the different measures in the residential buildings for the *Min Cost* scenario in 2050.

Together, the energy-related refurbishment measures account for 97.2 billion Euro while more than half of them

are determined by the walls. The occupancy control systems have a relatively high share with 12.8 billion Euro, followed by the windows and the roofs. One reason for the relatively small cost share of the efficiency measures is that most measures are chosen for buildings that are anyway in the refurbishment cycle due to their lifetime. Therefore, the costs for the sole efficiency measures are relatively small because installation costs, such as scaffolding construction, are seperately considered for these buildings.

The overall results are aggregated from the optimal system design of the different archetype buildings, whose cost structure is illustrated in Figure 12. The total annual cost of the buildings is scaled by the number of households in the buildings to show different sizes of buildings on a similar scale. In order to expose patterns between the buildings, they are manually clustered into four groups based on their resulting supply system. The Single Family Houses (SFHs) are manually differentiated between those with and those without heat pumps, while the Multi Family Houses (MFHs) are distinguished between those with and without fuel cells.
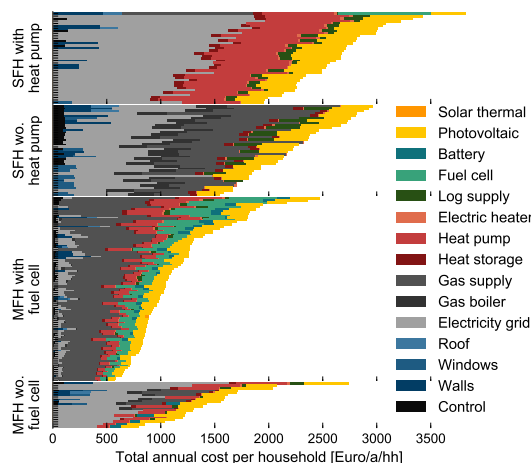
Figure 12: Cost composition of the different archetype buildings for the *Min Cost* scenario in 2050. They are grouped by Single-Family House (SFH) with and without (wo.) heatpumps and Multi-Family Houses (MFH) with and without (wo.) fuel cells.

In general, the only technology that is chosen for almost all of the buildings is rooftop photovoltaic. With the predicted small cost of the photovoltaic panels and high electricity price, these are in the cost-optimal solution for various scales but independent of the roof orientation of the building.

Except for one SFH that has a completely self-sufficient electricity supply, no other SFH has a fuel cell installed. Since the demand profile of a single-family house is highly volatile, the achievable full load hours for a self-sufficient electricity supply are too low for a fuel cell to become economically feasible. Furthermore, the required capacities of the fuel cell would be small, increasing the specific cost

due to a missing economy of scale.

Moreover, it is striking that the occupancy controllers are primarily installed in SFHs with gas boilers. The building cluster with gas boilers is dominated by compact buildings where only a few rooms need to be equipped with the thermostats, constituting small investment costs. Moreover, the heat capacity of those buildings is small and constitutes limited thermal inertia. This is beneficial for the occupancy controller, as the building can cool down and heat up faster in the case of vacant occupants. For large buildings with a high thermal mass, an occupancy controller only offers limited benefit.

All MFHs with a fuel cell have an additional heat pump installed. The cheap self-supply with electricity benefits electrical heat generation. Some of the MFHs add a battery system to increase the share of the photovoltaic and CHP electricity that can then be self-consumed.

The different full load hours and capacities of the technologies in the different archetype buildings are shown in Figure 13. The scale of the dots indicate how often the archetype buildings are assigned in total in Germany. In general, it can be seen that although photovoltaics are installed in all buildings, the achievable full load hours vary from 683 to 1025 depending on the roof orientation and location of the archetype building.

The highest full load hours are around 5000, and achieved by the fuel cells. It is observed that a larger fuel cell capacity correlates with higher achievable full load hours. This mainly relates to the occupancy profiles: due to statistical balancing effects, larger buildings have flatter profiles that can be covered by higher self-generation rates. Opposing effects are observed for the peak generators, such as the gas boiler with around 2000 full load hours and the electric heater with less than 1000 full load hours: the larger the installed capacities are, the smaller are the achievable full load hours. For the heat pump, no such effect is observed. It is operated with between 3000 and 4000 full load hours for small capacities as well as large ones.
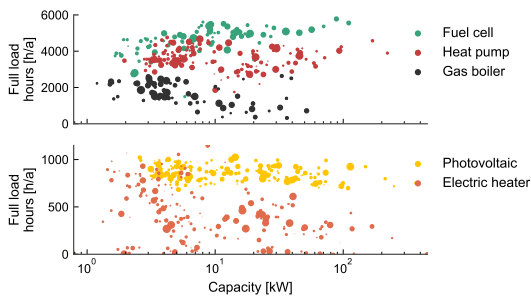

Figure 13: Full load hours and capacity of the installed technologies in the different archetype buildings for the *Min Cost* scenario in 2050. The size of the scatter is related to the overall appearance of the archetypes in Germany.

The distribution of scales and full load hours indicates that the heat pumps significantly rely on a peak boiler, since their scaling to the maximal heat load would be more

expensive. Nevertheless, it is open as to which peak boiler is chosen in the model. For a few full load hours, the electric heater is more cost-effective, while for many peak load hours an investment into a gas boiler could be advantageous. From a central infrastructure perspective, both options have an intrinsic economic issue, as they need the layout of an infrastructure that will be used in its maximal capacity for only a few hours per year.

4.2. Electricity grid load

The resulting electricity grid exchange, defined by the electricity imported for the heat pump, the conventional electricity demand, and the photovoltaic feed-in is illustrated in Figure 14. For comparison purposes, the grid exchange of the *Reference* scenario is shown as well. The aggregated electricity load of the *Reference* scenario is dominated by the occupant activities in the morning and evening. A small variation between winter and summer then appears. The overall load peaks in the evening hours during winter with 36.4 GW. This aggregated load significantly changes for the 2050 scenario, when during the summer the load demand is reduced to values below 10 GW, and also for the evening hours, while high daytime feed-in rates of the photovoltaic occur with up to 43.1 GW, exceeding the peak demand of the *Reference* scenario. The impact of the photovoltaic gets reduced during the winter but still reduces the load at noon for most days. The evening hours in winter are still the peak demand times with a load of up to 32.3 GW for the 2050 scenario, which is in a similar in magnitude to the *Reference* scenario.
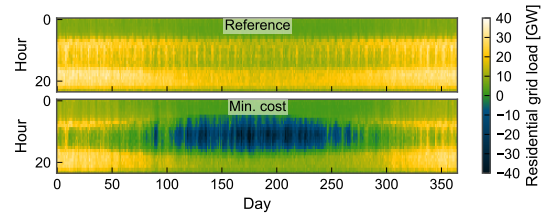

Figure 14: Aggregated grid exchange of the national residential building stock for the *Reference* and the *Min Cost* scenario.

As introduced previously, the technology installations depend on the building type. Therefore, the changes in the grid load also vary spatially depending on the local building topology, as illustrated in Figure 15. As expected, the majority of the regions reduce their annual electricity demand with the help of self-generation by photovoltaics and fuel cells. Nevertheless, regional differences are high: while urban areas are able to reduce their electricity demand by 60%, some rural areas even increase it. The high photovoltaic installations in rural areas are not sufficient to compensate for the increased electricity demand from the heat pumps. This effect intensifies for the case of the peak load, as almost no photovoltaic feed-in exists in the winter days, while the heat pumps are being operated in

full load. Therefore, regions characterized by large SFHs double their peak load. This is different for the urban areas that even reduce their peak load because the fuel cells exceed the electrical capacity of the heat pumps and are synchronously operated. Equivalent regional trends are observed for the feed-in: The rural areas feed up to 40% of the original electricity demand into the grid, while the urban areas have only small feed-in rates of 10%. Further, a gradient between north and south is recognizable due to the different solar irradiance.
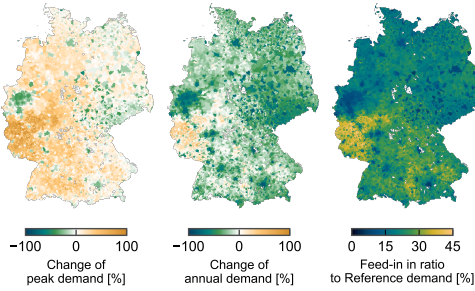

Figure 15: Spatial change of the peak electricity demand and the change of the cumulative positive demand from the *Reference* scenario to the *Min Cost* scenario. Furthermore, the amount of electricity feed-in to the grid in the *Min Cost* scenario is shown in ratio to the cumulative electricity demand in the *Reference* scenario.

In summary, the results indicate that the change of the energy supply in the rural areas is more challenging with respect to the electricity grid operation than the changes in the urban areas.

4.3. Value of analysis

In order to evaluate the robustness of the *Min Cost* scenario for 2050, 200 archetype buildings are again optimized, but parts of the technologies are excluded or forced into the solution space.

Figure 16 illustrates the aggregated resulting annual cost composition of the different cases that were considered for the analysis. Gas supply, fuel cell, photovoltaic, heat pump and refurbishment measures are each excluded from the solution space, and the other cost minimal solutions are compared to the original *Min Cost* scenario with all technologies available. The increase in the total systems costs can be interpreted as the *Value Of* the integration of a certain technology. As an additional case, the full package of refurbishment measures are enforced for all buildings that are in the refurbishment cycle in order to reach lower demands for space heating.

In case the fossil gas supply is excluded from the solution space, the electricity purchase doubles, as no fuel cells for self-consumption are installed. Bio-methane or another renewable fuel is too expensive in the considered scenario to replace the fossil gas in the fuel cells. Instead, higher capacities of photovoltaics are integrated into the solution, aggregating up to 160.3 GW. Moreover, the aggregated cost for heat pumps increases by 38% as their
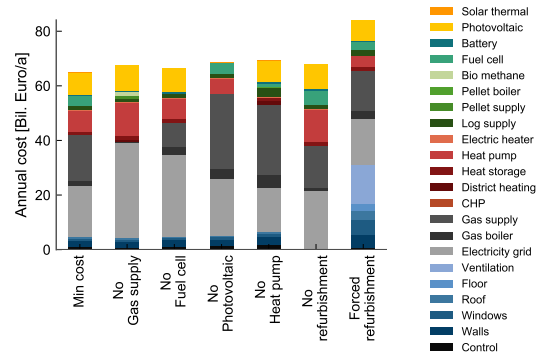

Figure 16: Annual cost of the *Min Cost* scenario and the resulting aggregated system cost if the solution space is constrained.

share of the heat supply increases. While the *Min Cost* solution did not include district heating or pellet boilers, they are used in small scales in the case that fossil gas is excluded. The amount of occupancy controllers is also reduced without fossil gas. The reason is that the heat pump is intensively used during the day in order to utilize photovoltaic electricity while heating up the building. Nevertheless, the occupancy controller lowers the comfort temperature especially during the day when the occupants are absent. These two temporally opposing effects reduce the value of an occupancy controller for the buildings supplied with heat pumps. The exclusion of fossil gas also constitutes the smallest GHG footprint that gets reduced from 51.9 Mt/a in the *Min Cost* scenario to 19.9 Mt/a, as shown in Figure 17.
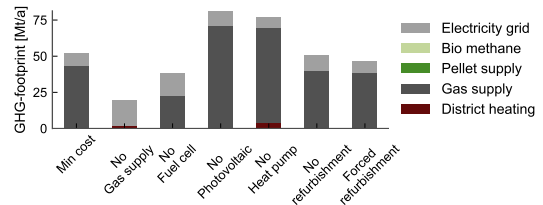

Figure 17: GHG footprint of the *Min Cost* scenario and the resulting aggregated GHG footprints if the solution space is constrained.

The structural changes to the *Min Cost* scenario are fairly small for the case that the fuel cell is excluded from the solution space. The net electricity import increases as in the previous scenario and compensates for the missing self-generation, but the photovoltaic capacities merely increase from 133.4 GW to 142.3 GW, while the heat pump capacities remain in a similar magnitude. This is different to the previous case and indicates that the value of further photovoltaic capacities is mainly correlated to higher heat pump capacities and not to smaller fuel cell capacities. The battery capacities are reduced from 16.9 GWh to 12.8 GWh, although the photovoltaic capacity is increasing. This implies that their operation partially comple-

11

ments the fuel cell operation.

Significant shifts and cost increases are recognizable in the case that the photovoltaic is excluded, while the electricity purchase only increases from 71.9 TWh/a to 80.9 TWh/a, the gas import almost doubles from 172.5 TWh/a to 285.7 TWh/a with the effect of a GHG footprint of up to 81.3 Mt/a. High gas boiler capacities compensate for the reduction of the heat pump capacities from 60.4 to 46.9 GW$_{th}$. This indicates the enforcing effect between the heat pump and the photovoltaic supply, which is economically advantageous in the case of self-consumption with photovoltaics is available. No battery capacities are installed, supporting the statement that their main economic driver for installation is the photovoltaic, although they are also partially used to increase the self-consumption with fuel cell electricity.

In the case that a heat pump is excluded from the solution space, the amount of gas increases by 113.2 TWh/a while the electricity demand only gets reduced by 13.5 TWh/a. In consequence, the GHG footprints increase by up to 76.0 Mt/a. Furthermore, the investment in refurbishment measures increases by 30%, dominated by more occupancy controller and more wall insulation and vice versa, indicating that especially cheap heat produced by the heat pumps lowers the motivation to invest in efficiency measures. Also, the fire wood supply increases from 21.2 TWh/a to 51.44 TWh/a, since it is a cheaper fuel than fossil gas in the scenario. Remarkable is the reduced investment in fuel cells, cutting their capacity from 12.7 to 5.1 GW$_{el}$. This illustrates that major fuel cell capacities are built to supply the heat pumps with electricity.

The exclusion of refurbishment measures from the solution space constitutes an increased investment in heat pumps and a reduced investment in gas boilers. This is surprising, as an enforcing effect between the heat pump and refurbishment measures could be expected because the refurbishment measures decrease the required supply temperature in the building, and vice versa, increasing the efficiency of heat pumps. Nevertheless, the economic effects predominate, the heat pumps have higher investment costs than the gas boilers, while on the other hand the operational energy cost for the gas supply is higher. In consequence, heat pumps are favored in the case of high heat demands and their deployment increases for the case of no refurbishment.

The reverse effect occurs for the forced refurbishment case: Installed heat pump capacities are reduced while gas boiler capacities increase. The overall demand for gas and electricity is reduced as the space heat demand drops to 209.1 TWh/a, in comparison to the 309.8 TWh/a in the *Min Cost* scenario and the 449 TWh/a in the *Reference* scenario. Nevertheless, the demand reduction is not able to compensate for the high cost of the refurbishment measures, resulting in an overall annual cost increase of 29.7%. In particular, ventilation systems with heat recovery amount to almost half of the efficiency measure costs. Ventilation systems do not benefit from the refurbishment
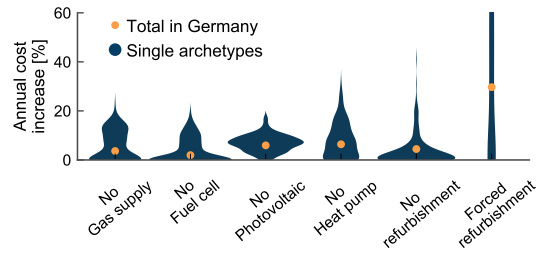

Figure 18: Annual cost increase for the case that certain technologies are excluded or added to the solution space in the *Min Cost* for 2050. The change is once shown for the total aggregated cost and once for the single archetype buildings.

cycle, as their integration cost in the building is mostly independent of any outside renovation measures. Also noticeable is the fact that the amount of occupancy control systems drops: If the heat demand is reduced anyway, additional measures such as temporally reducing the inner air temperature have a minor effect, making the occupancy controller economically unfavorable. The GHG footprint is only reduced to 45.1 Mt/a, which is much smaller than expected but explained by the switch of many buildings to gas boilers. This indicates a potential rebound effect that might occur in the future, in that the reduced demand for space heating lowers the economic incentive to invest in efficient but expensive heat supply technologies.

It is striking that the aggregated cost gain is moderate for all considered cases, except for the forced refurbishment case. This indicates that the prediction of the total cost is robust and not sensitive to the available technologies in the future, although, this robustness only accounts for an aggregated German-wide level, as illustrated in Figure 18. The figure shows the total cost increase and the distribution of the cost increase of the single buildings. While the total cost in Germany only increases by 3.65% for the case that no fossil gas supply is available, one of the archetype buildings has a 22.9% higher energy costs, while some other buildings are not affected at all, as they were also not supplied with gas in the *Min Cost* scenario. Similar effects are observed for the other sensitivity analyses: The sensitivities for single buildings are high, but the cost of the aggregated result is robust.

The impact on the electricity grid of the different cases is further illustrated in Figure 19. It shows the sorted grid load for the *Reference* scenario, the *Min Cost* scenario, and all related sensitivity analyses. The highest peak load occurs if the gas supply is completely excluded from the solution. No significant gas boiler capacities are able to satisfy the peak heat demand and no fuel cells can diminish the additional electricity load of the heat pumps. In consequence, the peak load almost doubles to 55.9 GW in comparison to the *Min Cost* scenario with 32.3 GW. The second highest demand is reached if no fuel cell is included and the peak load increases by 14.6 GW relative to the *Min Cost* scenario. This shows the importance

of decentralized flexible electricity generation in order to compensate for the increased electricity demand by the heat pumps. As is to be expected, the case without heat pumps has the lowest peak load, with 25.7 GW.
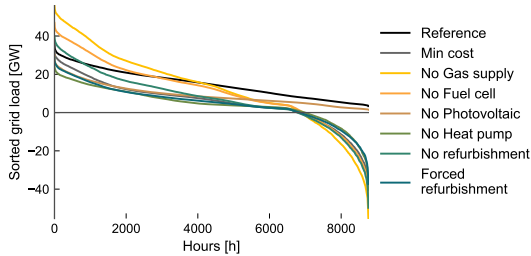

Figure 19: Sorted grid load of the *Min Cost* scenario and the grid load if the solution space is constrained.

The amount of photovoltaic feed-in is for all cases that include photovoltaics in a similar range. The maximal feed-in is reached with 55.4 GW for the exclusion of the gas supply, although the single buildings have the constraint to limit the feed-in to 50% of their maximal capacity.

5. Summary, conclusions and outlook

In this paper, a novel bottom-up model was introduced to predict the changing infrastructure and grid demand of residential buildings under different regulatory regimes and market environments. It is based on archetype buildings that represent a spatially-resolved building stock and individually optimize their energy supply structure to minimize their annual energy supply cost. The model was applied and validated for the residential building stock of Germany and a future scenario frame for 2050.

The main conclusions drawn from the future scenario are the following:

- The key technologies for reducing the GHG emissions in the building stock are photovoltaic and heatpumps that will significantly increase the seasonal variation of the residential electricity load, as their feed-in and demand temporally disjoin, resulting in a doubling of the peak electricity load in the winter hours in rural areas.

- The urban areas can compensate the increasing electricity demand by efficient co-generation units, e.g., in form of fuel cells, which cannot achieve sufficient economies of scale in single family houses in the rural areas.

- Significant amounts of photovoltaic electricity (for Germany up to 90 TWh/a) can be self-consumed while the majority is used for internal heat supply applications. Batteries are hardly deployed, as the heat applications provide enough flexibility for self-consumption.

- Refurbishment measures are expensive and only chosen in cases when the building is in the cosmetic refurbishment cycle. Therefore, space heat demand only decreases by 30% from 2015 to 2050 in the scenario. Instead, a shift towards an efficient integrated energy supply system, e.g. combinations of fuel cells with heat pumps, is favored.

The impacts on the peak and feed-in values are operation related to the scenario for 2050. They can be controlled by the different tariff structure, that could give incentives to shift consumption in time in order to flatern the load profile. Therefore, upcoming works should apply the model to different regulatory regimes and market environments and feed the results into grid models in order to determine an economically optimal market design.

Furthermore, the algorithm should be transferred to other energy sectors to derive spatially-distributed sector specific representatives. Thus, a cross-sectoral spatially resolved bottom-up model can be derived that respects the individual economic entities.

Acknowledgments

Appendix A. Techno-economic assumptions

The main input assumptions to parametrize the optimization models are introduced in the following section, e.g. residential energy prices and efficiencies of the different technologies. Section Appendix A.1 defines the parameters for the year 2015, while Appendix A.2 extends and adapts them to the year 2050.

Appendix A.1. Assumptions for 2015

In order to achieve a valid comparison of today's residential energy supply to the changes that will occur in the future, a valid scenario framework is introduced that represents today's cost and operation parameters for the residential energy supply systems.

The economic parameters considered for the supply technologies are illustrated in Table A.1, while their detailed derivation is discussed in Kotzur [64]. The structure of the investment costs is oriented around the cost model introduced in Lindberg et al. [38]. It differentiates between the fixed investment costs that occur in the case of installation and the specific investment costs that are added and related to the scale of the installations.

Although the model allows for the modeling of different interest rates for different building types to take into account of the different investment behavior of the building

13

Table A.1: Assumed economic parameters of the energy supply technologies for the *Reference* scenario.

Technology	CAPEX fix	CAPEX specific	OPEX %CAPEX/a	Lifetime a	Source
Gas boiler	2800 Euro	100 Euro/kW$_{th}$	1.5	20	[64]
Oil boiler	2800 Euro	100 Euro/kW$_{th}$	1.5	20	[64]
Pellet boiler	10000 Euro	300 Euro/kW$_{th}$	3.0	20	[64]
Heat pump	5000 Euro	600 Euro/kW$_{th}$	2.0	20	[64]
Heat storage	800 Euro	1200 Euro/m^3	0.0	25	[64]
Photovoltaic	1000 Euro	1400 Euro/kW$_{el}$	1.0	20	[64]
IC CHP	15000 Euro	1000 Euro/kW$_{el}$	7.0	15	[64]
Solar thermal	4000 Euro	350 Euro/m^2	1.0	20	[64]
Electric heater	0 Euro	60 Euro/kW$_{th}$	2.0	30	[38]

owners [81], it is here simplified to a single interest rate of 3%, which lays between the 2% to 5% considered in the literature [33, 38, 48, 82, 83].

The energy and resource prices are illustrated in Table A.2. The majority of the prices are derived from the study *Energieeffizienzstrategie Gebäude* [15, 84]. Their assumptions define the basic scenario framework for this thesis and rely themselves on the *Energiereferenzprognose* [85]. The majority of the resource prices assumed in the study align with the energy prices observed for 2016 [18, 86]. Nevertheless, the assumed gas price overshoots the observed price of 2016 by more than 1 ct/kWh, and was adapted in this work to the values reported for 2016 by the Bundesnetzagentur [86].

The GHG footprint includes the emissions of the previous conversion processes, such as in the extraction of fuels, or the GHG emissions of the German power plant mix.

Table A.2: Assumed residential energy prices including taxes, levies, and network charges based on *Energieeffizienzstrategie Gebäude* [15, 84, 85]. While missing parameters are derived from Lindberg et al. [87], KWKG [88], EEG [89]. The gas price is corrected to the observed gas prices in 2016 [86]. The GHG footprint and primary energy factors (PE) are taken from prognos [84]. FiT refers to Feed-in Tariff.

Technology -	OPEX-var Euro/kWh	OPEX-fix Euro/a	GHG kg/kWh	PE kWh/kWh	Comment -
Electricity supply	0.246	170	0.525	1.8	0.292 Euro/kWh for 3700 kWh/a
Gas supply	0.065	0	0.250	1.1	
Oil supply	0.064	0	0.320	1.1	
Pellet supply	0.060	0	0.014	0.2	
Heat pump tariff	0.190	70	0.525	1.8	
FiT CHP	-0.08	0	0.000	2.8	for less than 50 kWel
FiT PV	-0.108	0	0.000	1.8	
District heating	0.074	327	0.270	0.7	0.096 Euro/kWh for 15.000 kWh/a
Log supply	0.050	0	0.000	0.2	

Furthermore, the price structure is modified from a sole energy price (Euro/kWh) structure to a combination of a flat price (Euro/a) and an energy price (Euro/kWh). This is important because the savings due to self-consumption, e.g. of photovoltaic electricity, would be overestimated with the sole energy price. Additionally, this structure respects that specific wholesale prices decrease with larger energy consumptions rates [86].

The technical performance of the technologies is sum-

marized in Table A.3. The efficiencies are given for the Lower Heating Value (LHV) of gas, oil or pellets. The electrical and thermal CHP efficiencies are defined for a fixed operation ratio and cannot be varied in between. The values are chosen such that the different age structures of the technologies are respected, e.g. an efficiency is assumed for the gas boiler that refers to the efficiency of condensing boilers, while for the oil boiler a lower efficiency is considered that is related to older boiler technologies.

Table A.3: Summary of the main technical parameters of the energy supply technologies

Technology	Efficiency	Comment and *Reference*
Gas boiler	0.96	Condensing boiler [90]
Oil boiler	0.84	[91]
Pellet boiler	0.9	[38]
Heat pump	dynamic	[64] quality grade of 0.4
Heat storage	0.99	charge [38]
	0.99	discharge
	0.6%/h	self-discharge [92]
Photovoltaic	0.15%	based on Hanwha HSL 60 S [93] with 7 m^2/kWp
IC CHP	0.6	thermal [94]
	0.25	electric [94]
Electric heater	0.98	[91]
Solar thermal	dynamic	[38]
Fireplace	0.83	[91, 95]

The comfort temperature inside the buildings is assumed to have a value of 21°C for when occupants are active at home. The night reduction temperature is set for all buildings to 18°C.

Appendix A.2. Assumptions for 2050

The techno-economic assumptions for the future energy supply through 2050 are introduced in the following section. While many parameters are estimated to stay at a similar magnitude as in the *Reference* case in Section Appendix A.1, this section describes only the assumptions that are changing for the case of 2050. All prices and costs are provided as real prices in 2015.

While no major changes are expected for conventional heat generators, further learning rates and cost reductions are considered for photovoltaic and electrochemical technologies, as shown in Table A.4. Their detailed derivation and discussion is also performed in Kotzur [64].

Table A.4: Change and addition of economic parameters of the energy supply technologies for the year 2050.

Technology	CAPEX fix	CAPEX specific	OPEX %CAPEX/a	Lifetime a	Source
Photovoltaic	1000 Euro	650 Euro/kW$_{el}$	1.0	20	[64]
Battery	1000 Euro	300 Euro/kWh	2.0	15	[64]
Fuel cell	4000 Euro	1500 Euro/kW$_{el}$	3.0	15	[64]

The technical assumptions for 2050 are shown in Table A.5. The efficiency of the heat pumps is expected to increase further in the future [96], for which this work assumes an increase of the quality grade to 0.45, which is the upper bound of today's systems [64]. The photovoltaic efficiency is assumed to increase to a value of 30% [23]. Primarily, this impacts the space coverage on the rooftop and increases the photovoltaic potential that can be installed. The technical parameters of the batteries are derived from a prediction until 2050 [97], but some of today's residential storage systems already achieve similar efficiencies [98].

Table A.5: Summary of the main technical parameters of the energy supply technologies for 2050.

Technology	Efficiency	Comment and *Reference*
Heat pump	dynamic	[64]
		quality grade of 0.45
Photovoltaic	0.3	average 2050 [23]
		with 3.5 m²/kWp
Battery	0.95	charge [97]
	0.95	discharge [97]
	0.01%/h	self-discharge [97]
	0.5 kW/kWh	capacity factor
Fuel cell	0.33	thermal [64]
	0.52	electric [64]

The electrical efficiency of the fuel cell is assumed to be 52% and positions itself between the efficiency that can be achieved from Solid Oxide Fuel Cell (SOFC) systems and the efficiency of the Proton Exchange Membrane Fuel Cells (PEMFC), as discussed in detail in Kotzur [64]. A fully flexible operation is assumed for the year 2050. The efficiencies are considered to be the same for natural gas, biogas or hydrogen as potential alternative fuels [99].

The energy prices for 2050 are shown in Table A.6 and also rely on the *Energieeffizienzstrategie Gebäude* [15, 84] and *Energiereferenzprognose* [85]. The *Energiereferenzprognose* considers a carbon price of 76 Euro/ton for the year 2050, which, e.g., increases the gas price by 1.9 ct/kWh.

Furthermore, a bio-methane purchase is integrated with a price of 13.8 ct/kWh, which can be either a synthetic gas or biogas. As no sufficient predictions for bio-methane prices in 2050 are te be found, its price is derived from the production cost of bio-methane for the feed-in into the gas grid of 7.5 ct/kWh in 2013 [100], plus the surcharge for grid fees, tax etc. This surcharge is considered to be 6.3 ct/kWh, which is the difference between the gas market price of 3.3 ct/kWh and the residential gas price of 9.6 ct/kWh in 2050 [85]. All in all, it results in a price of 13.8 ct/kWh for the bio-methane, which is significantly above the fossil gas price.

No values for future feed-in tariffs were identified. There-

Table A.6: Assumed energy prices, GHG footprints and primary energy factors (PE) based on the *Energieeffizienzstrategie Gebäude* [15, 84, 85] for 2050.

Technology	OPEX-var	OPEX-fix	GHG	PE	Comment
-	Euro/kWh	Euro/a	kg/kWh	kWh/kWh	-
Electricity supply	0.220	170	0.122	0.4	0.266 Euro/kWh for 3700 kWh/a
Gas supply	0.096	0	0.250	1.1	
Bio-methane	0.138	0	0.014	0.2	
Oil supply	0.124	0	0.320	1.1	
Pellet supply	0.080	0	0.014	0.2	
HP Tarif	0.190	70	0.122	0.4	
FiTCHP	-0.010	0	0.000	0.4	
FiTPV	-0.010	0	0.000	0.4	
District heating	0.085	327	0.144	0.5	0.107 Euro/kWh for 15000 kWh/a
Log supply	0.065	0	0.000	0.2	

fore, the feed-in is only marginally subsidized, as it is highly dependent on the future market environment. A marginal value of 0.01 eur/kWh is chosen in order to guarantee that photovoltaic generation is not curtailed and is instead fed-in to the grid.

The cost and energetic impact of the refurbishment measures for the opaque building envelope are shown in Table A.7.

Table A.7: Techno-economic assumptions for the insulation measures of a single building. The two measure levels are derived from Schütz et al. [48] while the exact cost and lambda are taken from BMVBS [101].(* thickness equivalent. ** capital expenditures related only to energetic measures.)

Component	Measure	Thickness*	Lambda	CAPEX	CAPEX energy **
-		m	W/m/K	Euro/m²	Euro/m²
Wall	Base	0.15	0.035	124.0	51.5
	Future	0.22	0.035	140.9	68.5
Roof	Base	0.24	0.035	237.6	53.0
	Future	0.36	0.035	270.0	79.6
Floor	Base	0.08	0.035	51.7	-

All measures are additional layers to the existing envelope of the building. The costs are average values taken from a survey about subsided refurbishment measures in Germany [101]. They differ between the entire CAPEX of a refurbishment measure and the sole additional CAPEX of energy efficiency measures if the building would have been refurbished anyway, as discussed in Kotzur [64]. The costs relate to the exterior surface area of the building component. Two levels of potential insulation measures are considered and differ by the thickness of the insulation layer, and are referred to as *Base* and *Future*.

The costs of replacing the windows and changing the solar and thermal transmittance of the different window types are shown in Table A.8 and rely on the BMVBS [101] as well. The costs are specific to the window area of the building. Again, a differentiation is made between the *Base* and *Future* levels.

All envelope measures have a lifetime of 40 years with zero operational costs.

Table A.8: Techno-economic assumptions for the windows. The transmittance are based on [48] and the cost based on [101]

Measure	Solar transmittance -	Thermal transmittance $W/m^2/K$	CAPEX $Euro/m^2$
Base	0.575	1.1	313
Future	0.5	0.7	361.5

In addition to the conventional refurbishment measures at the envelope of the building, a heat recovery for the ventilation is assumed with a specific investment of 65 $Euro/m^2$ per living area, a lifetime of 25 years and operational cost of 4% per year according to the BMVBS [101] as a ratio to the original investment. If integrated, 80% of the heat losses due to ventilation would be recovered.

Lastly, an occupancy controller can be installed that reduces the comfort temperature in case of vacant occupants [64]. Based on the cost of Controme [102], they are assumed with a fixed investment of 1000 Euro for the central system controller and 3 $Euro/m^2$ per living area for the different thermostats in the rooms, including their installation costs. A lifetime of 15 years is assumed.

Appendix B. Supplementary results

The composition of the total annual residential energy cost for the *Min Cost* scenario in 2050 scenario are shown in Figure B.20.
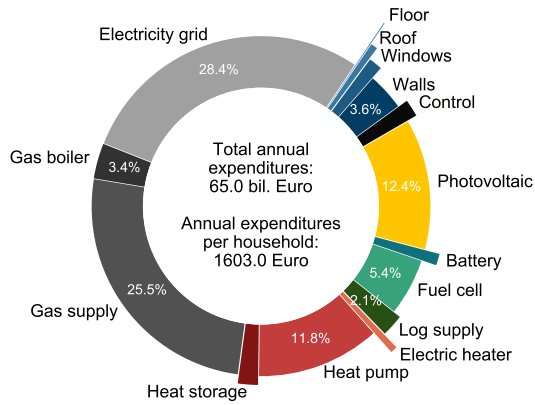

Figure B.20: Composition of the total annual costs over the whole of Germany for the *Min Cost* scenario in 2050.

The aggregated annual energy flows between the different considered system components are listed in Table B.9 for the different scenarios in 2050.

Table B.10 shows the aggregated installed capacities for all residential buildings for the different sensitivity cases.

Table B.9: Aggregated energy flows [TWh/a] between the different technologies for *Value of* analysis.

	Min Cost	No Gas supply	No Fuel cell	No Photovoltaic	No Heat pump	No refurbishment	Forced refurbishment
AC Node to Battery	5.2	2.0	3.7	0.0	5.1	6.1	5.2
AC Node to Building	112.8	112.8	112.8	112.8	112.8	112.8	112.8
AC Node to Electric heater	40.8	56.1	43.3	4.6	48.1	45.0	40.0
AC Node to Heat pump	34.3	26.9	16.2	24.6	0.0	50.1	21.0
AC Node to Hot water	6.8	6.8	6.8	6.8	6.8	6.8	6.8
Battery to AC Node	4.7	1.8	3.3	0.0	4.6	5.5	4.7
CHP to AC Node	0.0	0.0	0.2	0.0	0.0	0.0	0.0
Cool supply to Building	19.8	21.4	19.6	19.0	18.5	29.0	31.6
Electricity supply to AC Node	51.5	100.5	84.7	63.5	57.7	47.3	52.7
Fuel cell to AC Node	53.9	0.0	0.0	85.3	20.1	69.1	45.7
Gas supply to CHP	0.0	0.0	0.7	0.0	0.0	0.0	0.0
Gas supply to Fuel cell	103.7	0.0	0.0	164.1	38.6	132.9	87.9
Gas supply to Gas boiler	68.7	0.0	91.2	121.6	226.6	26.8	65.7
HP Tarif to Heat pump	20.4	46.2	40.2	17.4	0.0	42.1	10.5
Log supply to Fire place	21.2	19.4	23.0	23.6	51.4	21.3	25.8
Pellet supply to Pellet boiler	0.0	10.3	0.0	0.0	3.1	0.0	0.0
Renewable gas to Gas boiler	0.0	8.7	0.0	0.0	0.0	0.0	0.0
Heat pump to Building	225.1	296.5	231.0	169.5	0.0	363.9	126.7
CHP to HNode	0.0	0.0	0.4	0.0	0.0	0.0	0.0
District heating to HNode	0.0	7.9	0.8	0.0	15.0	0.0	0.0
Electric heater to HNode	40.0	55.0	42.5	4.5	47.1	44.1	39.2
Fire place to HNode	17.6	16.1	19.1	19.6	42.7	17.7	23.9
Fuel cell to HNode	34.2	0.0	0.0	54.2	12.7	43.9	29.0
Gas boiler to HNode	66.0	8.3	87.6	116.7	217.5	25.7	63.1
HNode to Building	84.7	23.4	78.1	123.3	265.8	57.4	82.4
HNode to Hot water	69.2	69.2	69.2	69.2	69.2	69.2	69.2
Pellet boiler to HNode	0.0	9.3	0.0	0.0	2.8	0.0	0.0
HNode to Heat storage	54.5	41.8	38.3	77.2	52.2	59.6	52.9
Heat storage to HNode	50.5	37.8	35.2	74.5	49.2	54.8	49.3
Photovoltaic to AC Node	89.7	102.4	94.7	0.0	90.4	98.9	82.7
Photovoltaic to FiTPV	24.1	33.9	26.4	0.0	19.2	27.3	20.7
Solar thermal to HNode	0.1	0.0	0.0	0.1	0.1	0.0	0.0

Table B.10: Aggregated installed capacities of the different technologies for the *Value of* analysis.

	Min Cost	No Gas supply	No Fuel cell	No Photovoltaic	No Heat pump	No refurbishment	Forced refurbishment
Gas boiler [GW_{th}]	36.6	5.1	47.6	83.9	111.9	14.7	36.3
Oil boiler [GW_{th}]	0.0	0.0	0.0	0.0	0.0	0.0	0.0
CHP [GW_{el}]	0.0	0.0	0.0	0.0	0.0	0.0	0.0
District heating [GW_{th}]	0.0	7.5	0.9	0.0	13.1	0.0	0.0
Heat storage [GWh_{th}]	215.6	291.4	216.6	63.4	173.9	265.4	188.6
Heat pump [GW_{th}]	60.4	83.1	60.4	47.0	0.0	95.5	34.6
Electric heater [GW_{th}]	99.7	97.1	90.3	83.6	75.4	121.0	84.4
Solar thermal [GW_{th}]	0.2	0.0	0.0	0.2	0.2	0.0	0.0
Pellet boiler [GW_{th}]	0.0	2.4	0.0	0.0	0.8	0.0	0.0
Battery [GWh_{el}]	16.9	7.1	12.8	0.0	17.1	20.0	17.4
Fuel cell [GW_{el}]	12.7	0.0	0.0	14.5	5.1	16.9	10.7
Photovoltaic [GW_{el}]	133.4	160.3	142.3	0.0	127.8	147.6	121.0

References

[1] IEA, CO2 Emissions from Fuel Combustion - 2015 Edition, Technical Report, International Energy Agency, 2015.

[2] AGEB, Auswertungstabellen zur energiebilanz deutschland 1990 bis 2016, 2017.

[3] RWI, Erstellung der Anwendungsbilanzen 2015 und 2016 für den Sektor der Privaten Haushalte und den Verkehrssektor in Deutschland, Technical Report, RWI Leibniz-Institut für Wirtschaftsforschung e.V., 2017.

[4] BMWi, Zahlen und Fakten Energiedaten, Technical Report, Bundesministerium für Wirtschaft und Energie, 2016.

[5] UN, Paris agreement - cop21, 2015.

[6] S. Solomon, G.-K. Plattner, R. Knutti, P. Friedlingstein, Irreversible climate change due to carbon dioxide emissions, Proceedings of the national academy of sciences 106 (2009) 1704–1709.

[7] EU, 2010. URL: https://eur-lex.europa.eu/legal-content/en/TXT/?uri=CELEX:32010L0031.

[8] EU, 2012. URL: http://eur-lex.europa.eu/legal-content/EN/TXT/PDF/?uri=CELEX:32012L0027&from=DE.

[9] REHVA, How to define nearly net zero energy buildings nZEB, Technical Report, 2011. URL: https://www.rehva.eu/fileadmin/hvac-dictio/03-2011/How_to_define_nearly_net_zero_energy_buildings_nZEB.pdf.

[10] A. J. Marszal, P. Heiselberg, J. S. Bourrelle, E. Musall, K. Voss, I. Sartori, A. Napolitano, Zero Energy Building –A review of definitions and calculation methodologies, Energy and Buildings 43 (2011) 971–979. doi:10.1016/j.enbuild.2010.12.022.

[11] J. OCallaghan, S. Mezger, M. Coughlin, K. Isles, A. Welsh, C. K. Lyttle, Utility of the future - A customer-led shift in the electricity sector, Technical Report, 2014.

[12] S. Agnew, P. Dargusch, Effect of residential solar and storage on centralized electricity supply systems, Nature Climate

Change 5 (2015) 315–318. doi:10.1038/nclimate2523.

[13] W. Rickerson, T. Couture, G. Barbose, D. Jacobs, G. Parkinson, E. Chessin, A. Belden, H. Wilson, H. Barrett, Residential prosumers - Drivers and policy options, Technical Report, 2014.

[14] R. McKenna, E. Merkel, D. Fehrenbach, S. Mehne, W. Fichtner, Energy efficiency in the German residential sector: A bottom-up building-stock-model-based analysis in the context of energy-political targets, Building and Environment 62 (2013) 77–88. doi:10.1016/j.buildenv.2013.01.002.

[15] BMWi, Energieeffizienzstrategie Gebäude, Technical Report, 2015.

[16] N. Diefenbach, T. Loga, B. Stein, Reaching the climate protection targets for the heat supply of the German residential building stock: How and how fast?, Energy and Buildings 132 (2016) 53–73. doi:10.1016/j.enbuild.2016.06.095.

[17] Beuth, Ableitung eines Korridors für den Ausbau der erneuerbaren Wärme im Gebäudebereich, Technical Report, Beuth Hoschule für Technik, ifeu - Institut für Energie- und Umweltforsschung Heidelberg GmbH, 2017.

[18] BMWi, Energiedaten - Tabelle 30: Internationaler Preisvergleich, Technical Report, 2018. URL: https://www.bmwi.de/Redaktion/DE/Binaer/Energiedaten/energiepreise-und-Energiekosten/energiedaten-energiepreise-5-xls.xls?__blob=publicationFile&v=17.

[19] M. Robinius, A. Otto, P. Heuser, L. Welder, K. Syranidis, D. Ryberg, T. Grube, P. Markewitz, R. Peters, D. Stolten, Linking the Power and Transport Sectors—Part 1: The Principle of Sector Coupling, Energies 10 (2017). doi:10.3390/en10070956.

[20] IWES, Interaktion EE-Strom, Wärme und Verkehr, Technical Report, Fraunhofer-Institut für Windenergie und Energiesystemtechnik (Fraunhofer IWES), 2015. URL: https://www.iee.fraunhofer.de/content/dam/iwes-neu/energiesystemtechnik/de/Dokumente/Veroeffentlichungen/2015/Interaktion_EEStrom_Waerme_Verkehr_Endbericht.pdf.

[21] UBA, Datenbasis zur Bewertung von Energieeffizienzmaßnahmen in der Zeitreihe 2005 –2014, Technical Report, Umweltbundesamt, 2017.

[22] H. Lund, A. N. Andersen, P. A. Østergaard, B. V. Mathiesen, D. Connolly, From electricity smart grids to smart energy systems –A market operation based approach and understanding, Energy 42 (2012) 96–102. doi:10.1016/j.energy.2012.04.003.

[23] ISE, Current and Future Cost of Photovoltaics. Long-term Scenarios for Market Development, System Prices and LCOE of Utility-Scale PV Systems, Technical Report, Study on behalf of Agora Energiewende, 2015.

[24] B. Nykvist, M. Nilsson, Rapidly falling costs of battery packs for electric vehicles, Nature Climate Change 5 (2015) 329–332. doi:10.1038/nclimate2564.

[25] C. Breyer, A. Gerlach, Global overview on grid-parity, Progress in Photovoltaics: Research and Applications 21 (2013) 121–136. doi:10.1002/pip.1254.

[26] K. Mainzer, K. Fath, R. McKenna, J. Stengel, W. Fichtner, F. Schultmann, A high-resolution determination of the technical potential for residential-roof-mounted photovoltaic systems in Germany, Solar Energy 105 (2014) 715–731. doi:10.1016/j.solener.2014.04.015.

[27] ISI, Netzentwicklungsplan Strom - Entwicklung der regionalen Stromnachfrage und Lastprofile, Technical Report, Fraunhofer-Institut für System- und Innovationsforschung, 2016.

[28] M. G. Beer, Regionalisiertes Energiemodell zur Analyse der flexiblen Betriebsweise von Kraft-Wärme-Kopplungsanlagen, Thesis, 2012.

[29] P. Seljom, K. B. Lindberg, A. Tomasgard, G. Doorman, I. Sartori, The impact of Zero Energy Buildings on the Scandinavian energy system, Energy 118 (2017) 284–296. doi:10.1016/j.energy.2016.12.008.

[30] P. Balcombe, D. Rigby, A. Azapagic, Investigating the importance of motivations and barriers related to microgeneration uptake in the UK, Applied Energy 130 (2014) 403–418. doi:10.1016/j.apenergy.2014.05.047.

[31] M. Achtnicht, R. Madlener, Factors influencing German house owners'preferences on energy retrofits, Energy Policy 68 (2014) 254–263. doi:10.1016/j.enpol.2014.01.006.

[32] C. Milan, C. Bojesen, M. P. Nielsen, A cost optimization model for 100% renewable residential energy supply systems, Energy 48 (2012) 118–127. doi:10.1016/j.energy.2012.05.034.

[33] D. Lauinger, P. Caliandro, J. Van herle, D. Kuhn, A linear programming approach to the optimization of residential energy systems, Journal of Energy Storage 7 (2016) 24–37. doi:10.1016/j.est.2016.04.009.

[34] A. Ashouri, S. S. Fux, M. J. Benz, L. Guzzella, Optimal design and operation of building services using mixed-integer linear programming techniques, Energy 59 (2013) 365–376. doi:10.1016/j.energy.2013.06.053.

[35] E. D. Mehleri, H. Sarimveis, N. C. Markatos, L. G. Papageorgiou, Optimal design and operation of distributed energy systems: Application to Greek residential sector, Renewable Energy 51 (2013) 331–342. doi:10.1016/j.renene.2012.09.009.

[36] S. Fazlollahi, P. Mandel, G. Becker, F. Maréchal, Methods for multi-objective investment and operating optimization of complex energy systems, Energy 45 (2012) 12–22. doi:10.1016/j.energy.2012.02.046.

[37] H. Harb, J.-N. Paprott, P. Matthes, T. Schütz, R. Streblow, D. Müller, Decentralized scheduling strategy of heating systems for balancing the residual load, Building and Environment 86 (2015) 132–140. doi:10.1016/j.buildenv.2014.12.015.

[38] K. B. Lindberg, G. Doorman, D. Fischer, M. Korpås, A. Ånestad, I. Sartori, Methodology for optimal energy system design of Zero Energy Buildings using mixed-integer linear programming, Energy and Buildings 127 (2016) 194–205. doi:10.1016/j.enbuild.2016.05.039.

[39] G. Cardoso, M. Stadler, S. Mashayekh, E. Hartvigsson, The impact of ancillary services in optimal DER investment decisions, Energy 130 (2017) 99–112. doi:10.1016/j.energy.2017.04.124.

[40] T. Schütz, M. H. Schraven, S. Remy, J. Granacher, D. Kemetmüller, M. Fuchs, D. Müller, Optimal design of energy conversion units for residential buildings considering German market conditions, Energy 139 (2017) 895–915. doi:10.1016/j.energy.2017.08.024.

[41] M. Hamdy, A. Hasan, K. Siren, A multi-stage optimization method for cost-optimal and nearly-zero-energy building solutions in line with the EPBD-recast 2010, Energy and Buildings 56 (2013) 189–203. doi:10.1016/j.enbuild.2012.08.023.

[42] R. Evins, Multi-level optimization of building design, energy system sizing and operation, Energy 90 (2015) 1775–1789. doi:10.1016/j.energy.2015.07.007.

[43] M. Stadler, G. Cardoso, S. Mashayekh, T. Forget, N. DeForest, A. Agarwal, A. Schönbein, Value streams in microgrids: A literature review, Applied Energy 162 (2016) 980–989. doi:10.1016/j.apenergy.2015.10.081.

[44] X. Han, H. Zhang, X. Yu, L. Wang, Economic evaluation of grid-connected micro-grid system with photovoltaic and energy storage under different investment and financing models, Applied Energy 184 (2016) 103–118. doi:10.1016/j.apenergy.2016.10.008.

[45] R. Streblow, K. Ansorge, Genetischer Algorithmuszur kombinatorischen Optimierung von Gebäudehülle und Anlagentechnik, Technical Report, 2017.

[46] R. Wu, G. Mavromatidis, K. Orehounig, J. Carmeliet, Multi-objective optimisation of energy systems and building envelope retrofit in a residential community, Applied Energy 190 (2017) 634–649. doi:10.1016/j.apenergy.2016.12.161.

[47] M. Stadler, M. Groissböck, G. Cardoso, C. Marnay, Optimizing Distributed Energy Resources and building retrofits with the strategic DER-CAModel, Applied Energy 132 (2014) 557–

567. doi:10.1016/j.apenergy.2014.07.041.

[48] T. Schütz, L. Schiffer, H. Harb, M. Fuchs, D. Müller, Optimal design of energy conversion units and envelopes for residential building retrofits using a comprehensive MILP model, Applied Energy 185 (2017) 1–15. doi:10.1016/j.apenergy.2016.10.049.

[49] M. Kavgic, A. Mavrogianni, D. Mumovic, A. Summerfield, Z. Stevanovic, M. Djurovic-Petrovic, A review of bottom-up building stock models for energy consumption in the residential sector, Building and Environment 45 (2010) 1683–1697. doi:10.1016/j.buildenv.2010.01.021.

[50] S. P. Corgnati, E. Fabrizio, M. Filippi, V. Monetti, Reference buildings for cost optimal analysis: Method of definition and application, Applied Energy 102 (2013) 983–993. doi:10.1016/j.apenergy.2012.06.001.

[51] É. Mata, A. Sasic Kalagasidis, F. Johnsson, Building-stock aggregation through archetype buildings: France, Germany, Spain and the UK, Building and Environment 81 (2014) 270–282. doi:10.1016/j.buildenv.2014.06.013.

[52] IWU, Deutsche Gebaeudetypologie. Systematik und Datensaetze, Technical Report, Institut Wohnen und Umwelt (IWU), 2005. URL: http://www.iwu.de/fileadmin/user_upload/dateien/energie/klima_altbau/Gebaeudetypologie_Deutschland.pdf.

[53] IWU, Datenbasis Gebäudebestand - Datenerhebung zur energetischen Qualität und zu den Modernisierungstrends im deutschen Wohngebäudebestand, Technical Report, Institut Wohnen und Umwelt Bremer Energie Institut, 2010.

[54] EPISCOPE, 2016. URL: http://episcope.eu/iee-project/episcope/.

[55] R. Hendron, C. Engebrecht, Building America Research Benchmark Definition, Technical Report, National Renewable Energy Laboratory, 2010. URL: https://www.nrel.gov/docs/fy10osti/47246.pdf.

[56] P. Torcellini, M. Deru, B. Griffith, K. Benne, Doe commercial building benchmark models, 2008.

[57] G. Dall'O', A. Galante, G. Pasetti, A methodology for evaluating the potential energy savings of retrofitting residential building stocks, Sustainable Cities and Society 4 (2012) 12–21. doi:10.1016/j.scs.2012.01.004.

[58] C. Cerezo, J. Sokol, C. Reinhart, A. Al-Mumin, 2015. URL: http://www.ibpsa.org/proceedings/BS2015/p2435.pdf.

[59] J. Sokol, C. Cerezo Davila, C. F. Reinhart, Validation of a Bayesian-based method for defining residential archetypes in urban building energy models, Energy and Buildings 134 (2017) 11–24. doi:10.1016/j.enbuild.2016.10.050.

[60] S. Fazlollahi, G. Becker, F. Maréchal, Multi-objectives, multi-period optimization of district energy systems: II-Daily thermal storage, Computers & Chemical Engineering 71 (2014) 648–662. doi:10.1016/j.compchemeng.2013.10.016.

[61] J. A. Fonseca, A. Schlueter, Integrated model for characterization of spatiotemporal building energy consumption patterns in neighborhoods and city districts, Applied Energy 142 (2015) 247–265. doi:10.1016/j.apenergy.2014.12.068.

[62] S. Bundesamt, 2011. URL: https://www.zensus2011.de/DE/Home/home_node.html.

[63] L. Welder, D. S. Ryberg, L. Kotzur, T. Grube, M. Robinius, D. Stolten, Spatio-temporal optimization of a future energy system for power-to-hydrogen applications in Germany, Energy 158 (2018) 1130–1149. doi:10.1016/j.energy.2018.05.059.

[64] L. Kotzur, Future Grid Load of the Residential Building Sector, Thesis, 2018. URL: http://juser.fz-juelich.de/record/858675.

[65] L. Kotzur, P. Markewitz, M. Robinius, D. Stolten, Impact of different time series aggregation methods on optimal energy system design, Renewable Energy 117 (2018) 474–487. doi:10.1016/j.renene.2017.10.017.

[66] D. EN ISO, Thermal performance and energy use in the build environment (ISO 13790:2008) (2008).

[67] E. McKenna, M. Thomson, High-resolution stochastic integrated thermal–electrical domestic demand model, Applied Energy 165 (2016) 445–461. doi:10.1016/j.apenergy.2015.12.089.

[68] I. Richardson, M. Thomson, D. Infield, C. Clifford, Domestic electricity use: A high-resolution energy demand model, Energy and Buildings 42 (2010) 1878–1887. doi:10.1016/j.enbuild.2010.05.023.

[69] I. Richardson, M. Thomson, D. Infield, A. Delahunty, Domestic lighting: A high-resolution energy demand model, Energy and Buildings 41 (2009) 781–789. doi:10.1016/j.enbuild.2009.02.010.

[70] I. Richardson, M. Thomson, D. Infield, A high-resolution domestic building occupancy model for energy demand simulations, Energy and Buildings 40 (2008) 1560–1566. doi:10.1016/j.enbuild.2008.02.006.

[71] R. W. Andrews, J. S. Stein, C. Hansen, D. Riley, Introduction to the Open Source PV-LIB for Python Photovoltaic System Modeling Package (2014).

[72] DIN, Din en 12831 - heating systems and water based cooling systems in buildings – method for calculation of the design heat load, 2014.

[73] DWD, Testreferenzjahre (TRY) (2012).

[74] C. Bollmeyer, J. D. Keller, C. Ohlwein, S. Wahl, S. Crewell, P. Friederichs, A. Hense, J. Keune, S. Kneifel, I. Pscheidt, S. Redl, S. Steinke, Towards a high-resolution regional reanalysis for the European CORDEX domain, Quarterly Journal of the Royal Meteorological Society 141 (2015) 1–15. doi:10.1002/qj.2486.

[75] L. Kotzur, P. Markewitz, M. Robinius, D. Stolten, Time series aggregation for energy system design: Modeling seasonal storage, Applied Energy 213 (2018) 123–135. doi:10.1016/j.apenergy.2018.01.023.

[76] T. Kannengießer, M. Hoffmann, L. Kotzur, P. Stenzel, P. Markewitz, F. Schütz, K. Peters, S. Nykamp, D. Stolten, M. Robinius, Reducing computational load for mixed integer linear programming: An example for a district and an island energy system (2019). URL: https://www.preprints.org/manuscript/201905.0116/download/final_file.

[77] B. Bahl, A. Kümpel, H. Seele, M. Lampe, A. Bardow, Time-series aggregation for synthesis problems by bounding error in the objective function, Energy 135 (2017) 900–912. doi:10.1016/j.energy.2017.06.082.

[78] Z. Huang, Extensions to the k-means algorithm for clustering large data sets with categorical values, 1998. URL: https://link.springer.com/content/pdf/10.1023/A:1009769707641.pdf.

[79] S. Lloyd, Least squares quantization in PCM, IEEE Transactions on Information Theory 28 (1982) 129–137. doi:10.1109/TIT.1982.1056489.

[80] A. K. Jain, Data clustering: 50 years beyond K-means, Pattern Recognition Letters 31 (2010) 651–666. doi:10.1016/j.patrec.2009.09.011.

[81] J. Schleich, X. Gassmann, C. Faure, T. Meissner, Making the implicit explicit: A look inside the implicit discount rate, Energy Policy 97 (2016) 321–331. doi:10.1016/j.enpol.2016.07.044.

[82] A.-L. Klingler, Self-consumption with PV + Battery systems: A market diffusion model considering individual consumer behaviour and preferences, Applied Energy 205 (2017) 1560–1570. doi:10.1016/j.apenergy.2017.08.159.

[83] A. Lahnaoui, P. Stenzel, J. Linssen, Techno-economic analysis of photovoltaic battery system configuration and location, Applied Energy (2017). doi:10.1016/j.apenergy.2017.09.093.

[84] prognos, Hintergrundpapier Energieeffizienzstrategie Gebäude, Technical Report, 2015.

[85] EWI, Entwicklung der Energiemaerkte - Energiereferenzprognose, Technical Report, On behalf of the Federal Ministry for Economic Affairs and Energy (BMWi), 2014.

[86] Bundesnetzagentur, Monitoringbericht 2017, Technical Report, 2017. URL: https://www.bundesnetzagentur.de/SharedDocs/Downloads/DE/Allgemeines/Bundesnetzagentur/

Publikationen/Berichte/2017/Monitoringbericht_2017.
pdf?__blob=publicationFile&v=4.

[87] K. B. Lindberg, D. Fischer, G. Doorman, M. Korpås, I. Sartori, Cost-optimal energy system design in Zero Energy Buildings with resulting grid impact: A case study of a German multi-family house, Energy and Buildings 127 (2016) 830–845. doi:10.1016/j.enbuild.2016.05.063.

[88] KWKG, Gesetz ür die erhaltung, die modernisierung und den ausbau der kraft-wärme-kopplung, 2016. URL: https://www.gesetze-im-internet.de/.

[89] EEG, Gesetz für den ausbau erneuerbarer energien, 2017. URL: https://www.gesetze-im-internet.de/.

[90] H.-M. Henning, A. Palzer, A comprehensive model for the German electricity and heat sector in a future energy system with a dominant contribution from renewable energy technologies—Part I: Methodology, Renewable and Sustainable Energy Reviews 30 (2014) 1003–1018. doi:10.1016/j.rser.2013.09.012.

[91] UBA, Klimaneutraler Gebäudebestand 2050 - Energieeffizienzpotentiale und die Auswirkungen des Klimawandels auf den Gebäudebestand, Technical Report, Umweltbundesamt, 2017. URL: https://www.umweltbundesamt.de/sites/default/files/medien/1410/publikationen/2017-11-06_climate-change_26-2017_klimaneutraler-gebaeudebestand-ii.pdf.

[92] T. Schütz, R. Streblow, D. Müller, A comparison of thermal energy storage models for building energy system optimization, Energy and Buildings 93 (2015) 23–31. doi:10.1016/j.enbuild.2015.02.031.

[93] B. H. King, C. W. Hansen, D. Riley, C. D. Robinson, L. Pratt, Procedure to Determine Coefficients for the Sandia Array Performance Model, Technical Report, Sandia National Laboratories, 2016.

[94] ASUE, BHKW-Kenndaten 2014/2015 - Module, Anbieter, Kosten, Technical Report, Arbeitsgemeinschaft für sparsamen und umweltfreundlichen Energieverbrauch e.V., 2015.

[95] Olsberg, Produktdatenblatt Olsberg Palena Cmpact, Technical Report, 2018. URL: https://www.olsberg.com/578912-wee-de-wAssets/docs/kaminoefen/palena-compact/anleitungen-zertifikate-ersatzteillisten/Produktdatenblatt_Palena-Compact_23-575_ohne-OEC.pdf.

[96] H. Willem, Y. Lin, A. Lekov, Review of energy efficiency and system performance of residential heat pump water heaters, Energy and Buildings 143 (2017) 191–201. doi:10.1016/j.enbuild.2017.02.023.

[97] P. Elsner, D. U. Sauer, Energiespeicher - Technologiesteckbrief zur Analyse "Flexibilitätskonzepte für die Stromversorgung 2050", Technical Report, 2015.

[98] K. Kairies, D. Haberschusz, J. v. Ouwerkerk, J. Strebel, O. Wessels, D. Magnor, J. Badeda, D. U. Sauer, Wissenschaftliches Mess- und Evaluierungsprogramm Solarstromspeicher - Jahresbericht 2016, Technical Report, Institut für Stromrichtertechnik und Elektrische Antriebe der RWTH Aachen, 2016.

[99] R. Peters, R. Deja, M. Engelbracht, M. Frank, V. N. Nguyen, L. Blum, D. Stolten, Efficiency analysis of a hydrogen-fueled solid oxide fuel cell system with anode off-gas recirculation, Journal of Power Sources 328 (2016) 105–113. doi:10.1016/j.jpowsour.2016.08.002.

[100] Bundesnetzagentur, Biogas- Monitoringbericht 2014, Technical Report, 2014. URL: https://www.bundesnetzagentur.de/SharedDocs/Downloads/DE/Sachgebiete/Energie/Unternehmen_Institutionen/ErneuerbareEnergien/Biogas/Biogas_Monitoring/Biogas_Monitoringbericht_2014.pdf?__blob=publicationFile&v=1.

[101] BMVBS, Kosten energierelevanter Bau- und Anlagenteile bei der energetischen Modernisierung von Wohngebäuden, Technical Report, 2012. URL: http://www.bbsr.bund.de/BBSR/DE/Veroeffentlichungen/BMVBS/Online/2012/DL_ON072012.pdf?__blob=publicationFile&v=2.

[102] Controme, Controme - Fußbodenheizung Set-Funk, Technical Report, 2018. URL: https://www.controme.com/produkt/fussbodenheizung-set-funk-2/.